





Seismic response of the Lengzhuguan slope during Kangding Ms5.8 earthquake

WANG Yun-sheng^{1*}  <http://orcid.org/0000-0002-1774-9494>;  e-mail: wangys60@163.com

HE Jian-xian^{1,2,3}  <http://orcid.org/0000-0002-4351-1068>; e-mail: hejianxian@mail.iggcas.ac.cn

LUO Yong-hong¹  <http://orcid.org/0000-0001-7462-1182>; e-mail: luoyonghong2012@cdut.cn

* Corresponding author

¹ State Key Laboratory of Geohazard Prevention and Geoenvironmental Protection, Chengdu University of Technology, Chengdu 610059, China

² Key Laboratory of Shale Gas and Geoenvironment, Institute of Geology and Geophysics, Chinese Academy of Sciences, Beijing 100029, China

³ University of Chinese Academy of Sciences, Beijing 100049, China

Citation: Wang YS, He JX, Luo YH (2017) Seismic response of the Lengzhuguan slope during Kangding Ms5.8 earthquake. Journal of Mountain Science 14(11). <http://doi.org/10.1007/s11629-017-4368-1>

© Science Press and Institute of Mountain Hazards and Environment, CAS and Springer-Verlag GmbH Germany 2017

Abstract: In order to investigate the role of the amplification of peak ground acceleration (PGA) in seismic landslide formation mechanisms and study how earthquake waves interact with rock structures, a few strong-motion seismometers are installed at various locations on both sides of the Lengzhuguan gully. Five strong-motion seismometers were triggered at different depths in a tunnel at the same altitude during the Kangding Ms 5.8 earthquake on November 25th, 2014. The data reveal that the horizontal peak acceleration (PGA_H) at each site decreased with increasing site depths. The PGA_H at the deepest monitoring site (99 m from the tunnel entrance) was approximately half that of the outermost site. The amplitude of the acceleration response spectrum was also attenuated from the entrance inwards, the dynamic magnification factor (β) of the standard acceleration spectrum was less than 3.5, and rate of change was the same as that for the amplitude acceleration response. The Fourier spectra of each monitoring site also decreased from the outside inwards, and the components of the Fourier spectra were more complex at the surface.

Keywords: Earthquake; Tunnel; Ground motion attenuation; Topographic effects; Lengzhuguan; Horizontal peak acceleration

Introduction

After the Wenchuan, Lushan and Ludian earthquakes occurring in the recent years in Southwest China, many Chinese scholars have been attracted to the study of the dynamic responses and stabilities of slopes under earthquake loading for geotechnical and geological engineering. The number of slope failures has been a key factor in the damage from high and steep slope geo-hazards in the cut slopes in western China, and the scale and size of the landslides or collapses correlate with the depths of the unstable rock masses. Topographic amplification is generally considered to be the main causal factor for these slope failures (Geli et al. 1988; Huang et al. 2013; Luo and Wang 2013; Luo et al. 2013). Monitoring the data revealed that topographic amplification was conspicuous at isolated ridges and slope breaks

Received: 13 January 2017

Revised: 15 February 2017

Accepted: 11 May 2017

(Wang et al. 2015; He et al. 2015). Based on the physical model tests of the Ertan arch dam, it was found that topographic amplification occurred both in the vertical and horizontal directions (Wang 1987; Wang and Wang 1987). The dynamic responses of different types of slopes have been studied through numerical simulation (Qi et al. 2003; Qi et al. 2007). However, the depths of the topographic amplification and the laws of their dynamic responses are poorly understood, and there is no good way to select appropriate ground motion parameters for potential slide surfaces at different depths. Hence, it is difficult to meet the significant slope-supporting engineering requirements for further design based on only one peak acceleration.

In the past few decades, the seismic responses of ground motion to the characteristics of depths below ground level has been studied to some degree due to the development of urban underground spaces. Some foreign scholars studied acceleration data from different vertical depths in earthquake zones with different soil foundations (Luo 1988). Based on the statistical data from 132 underground engineering damage cases, it was found that damage was reduced significantly at depths greater than 50 meters, and there was minimal damage at depths beyond 300 meters (Sharma et al. 1992). Damage to tunnels from the 5-12 Wenchuan earthquake was analyzed, and it was found that the degree of damage was slight to moderate when the horizontal depth was above 50 meters and was light or nonexistent when it was more than 100 meters in a hard rock tunnel (Li 2008). These previous studies indicate that the opening segment of the tunnel is where the emphasis should be placed for the mitigation of the destructive effects of earthquakes (Luo et al. 2008). The dynamic responses of a mountain tunnel have been analyzed by means of a large-scale shaking table test (Shen et al. 2009). Numerical stimulations were conducted to study the slope and tunnel stability under dynamic loadings (Zheng et al. 2010). To study the effect of the tunnel depth on the stability of its lining, the responses of a mountain tunnel at eight different depths to earthquake forcings were calculated using the finite element method (Jiang et al. 2014). These results contribute to a new way of studying the tunnel-entrance stability during earthquakes, but there is

still a lack of seismic monitoring data, and the homogeneous model materials make it difficult to simulate real situations in actual tunnels.

With the support of the China Geological Survey Bureau, the National Science Foundation of China and the State Key Laboratory of Geohazard Prevention and Geoenvironmental Protection, monitoring stations was installed on both sides of the Lengzhuguan ditch, Sichuan Province, southwestern China, in 2011 (Figure 1). At 23:19 November 25, 2014, an Ms 5.8 earthquake occurred in Kangding County, Sichuan, with an epicenter 43 km from the monitoring stations. Ten seismic instruments in this area were triggered by the earthquake, data series from #1, #2, #6-5 and #7-3 were obtained to study the topographic amplification factors and the monitoring data from the five instruments in the #6 adit were used to study the variations of the seismic responses from the outside surface to inside at different depths below the surface.

1 Study Area and Methods

The Lengzhuguan earthquake monitoring adit stations are located on both sides of Lengzhuguan river valley, near where it flows into the Dadu River on its right bank. Two stations are located on the right bank of the Lengzhuguan river valley, and five stations are located on the left bank (Figure 2). One seismic monitoring instrument was installed at each station, from 1 to 5, five monitoring instruments were included in station 6 and three were included in station 7 (each instrument is at a different distance from the entrance) (Figure 3). The ridge on the right bank reaches an elevation of 1520 m, while the left bank is a 1000 m high sloping terrain that is connected to the right concave bank of the Dadu River. Station 1 is at the top of the ridge on the right bank, and Station 2 is halfway up the ridge; Stations 3, 4 and 5 are situated at a slope break, and Stations 6 and 7 are located at different levels on the nearly rectilinear slope. The earthquake motions were measured by E-catcher strong-motion seismographs (made by Application of Japan's Saitama Prefecture, Saitama City, Minamiku Daitakubo 2-2-19), with the basic sensitivity parameters of 1 V/g, a meter full scale of 2000 gal (1 gal=1 cm·s⁻²), and the range of cycle

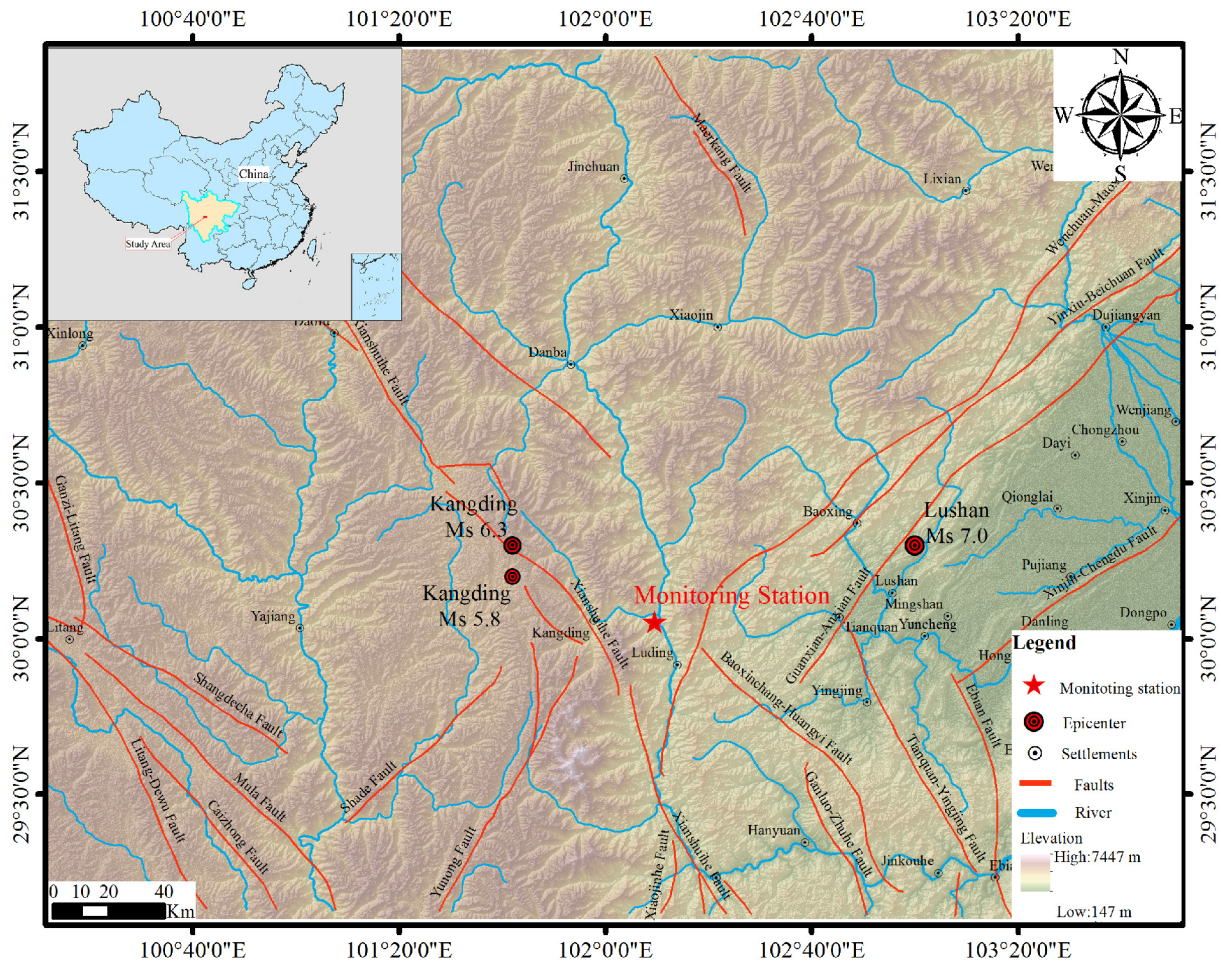


Figure 1 Geographic location of the monitoring section and the study area including three major earthquakes epicenter.

frequency is DC~20 Hz (-3 dB).

Geologically, the Lengzhuguan slope is located on the Sichuan-Yunnan rhombic block, and the left-lateral strike thrust Xianshuihe fault crosses study area. The main lithologic units are represented by granite and amphibolite (Lower Proterozoic).

2 Results

Ten of the monitoring instruments at different locations were triggered during the Kangding Ms 5.8 earthquake, and the seismic responses were obtained on both sides of the Lengzhuguan gully. The location parameters of the monitoring stations are given in Table 1.

To study the topographic amplification on both sides of the Lengzhuguan gully, monitoring

data are collected from #1, #2, #6-5 and #7-3. The attenuation effect could be eliminated with #6-5 and #7-3. The characteristics of the ground motion parameters of each of the monitoring stations are listed in Table 2.

At the Guza earthquake monitoring station (at a distance of 7 km from the Lengzhuguan monitoring section and located at the bottom of a valley that has almost the same lithological and topographical condition as the Lengzhuguan section), the horizontal and vertical components of the PGA of the main shock records are 12.3, 10.7 and 8.6 gal, respectively. Therefore, these monitoring data are used as reference values for the Lengzhuguan section because station 3, which was intended to provide the reference values for the bottom of the valley in the Lengzhuguan section, was not triggered in the Kangding Ms 5.8 earthquake.

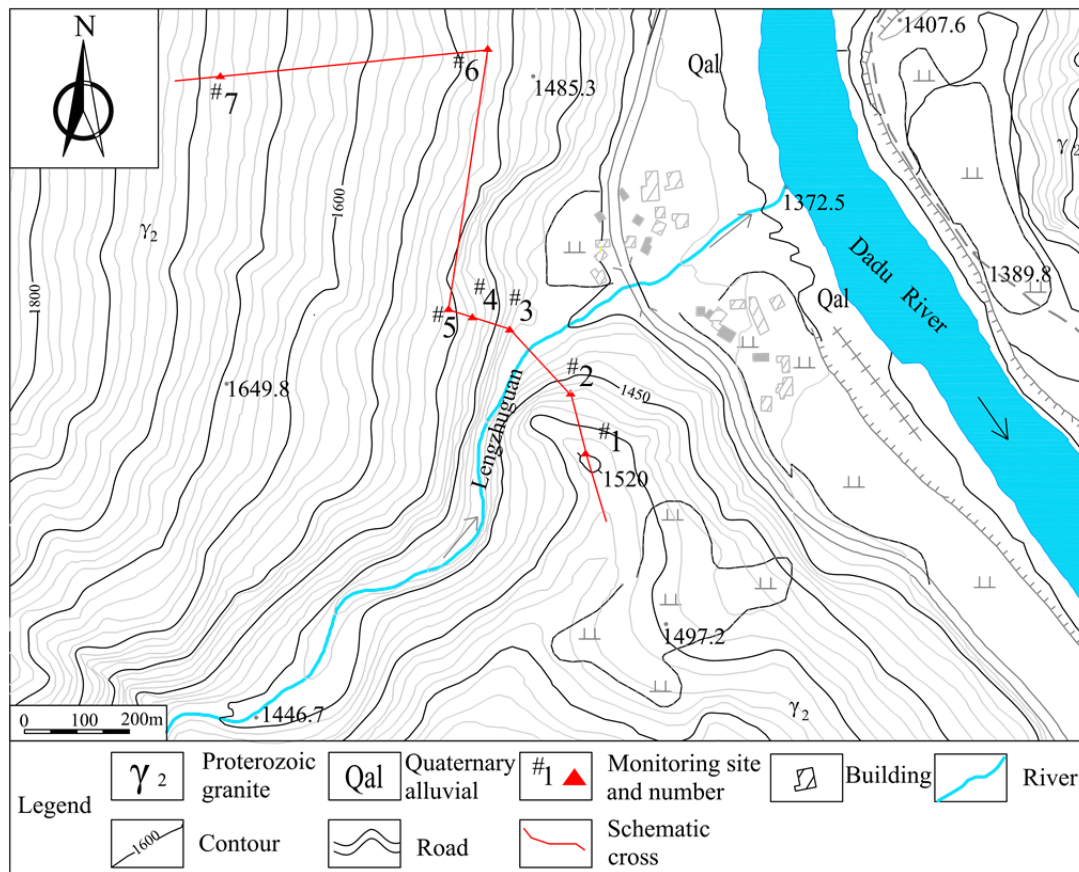


Figure 2 Topographic map of Lengzhuguan slope showing locations of the adits with seismic monitoring instruments.

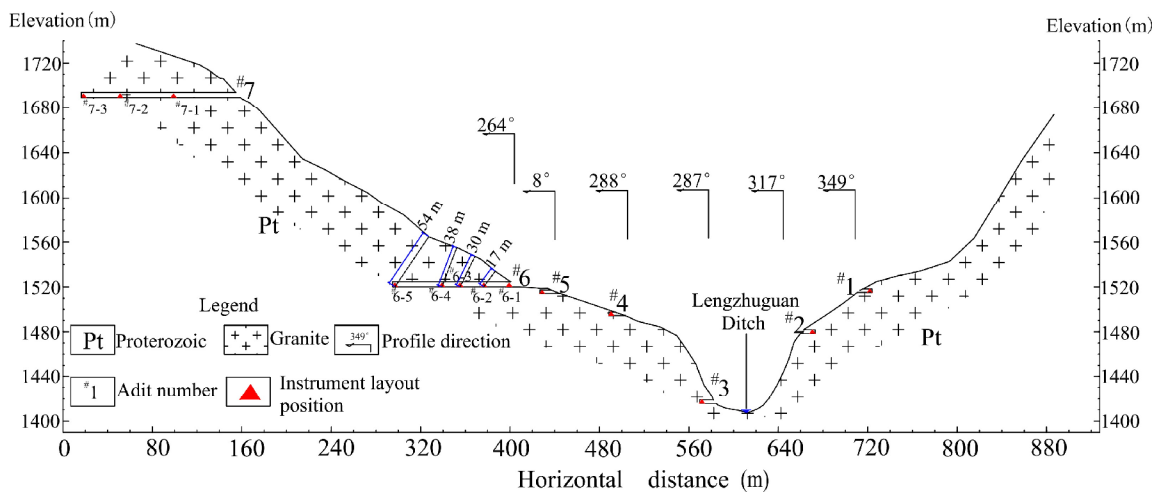


Figure 3 Lengzhuguan monitoring schematic cross-section.

The calculation results show that the PGA amplification factor of station 1 was more than that of 6 and that of station 2 was between 1.57 and 2.8. However, the amplification factors of #6-5 and #7-3 are approximately 1 in the horizontal direction, and the vertical are also below 2. Thus, the ground motion topographic amplification effect on the right side of the valley is stronger than that on the

left. From the Lengzhuguan hydropower station reconnaissance data, it can be concluded that both sides have almost the same lithologic and rock mass characteristics; therefore, the terrain conditions appear to be the key factors in the different topographic amplification effects. However, there is a thin Quaternary alluvial deposit around stations 1 and 2, which may

contribute to the seismic response amplification. Still, the previously mentioned soil effect can be omitted when compared with the magnitude of the steep crest topographic effect.

Table 1 The parameters of each monitoring site

Number	Elev. (m)	Epicentral distance (km)	Depth (m)	Lithology	Instrument
#1	1516	43.68	1	granite	E-catcher
#2	1478	43.65	1	granite	E-catcher
#6-1	1520	43.35	1	granite	Go1NET-3
#6-2			17		Go1NET-3
#6-3			30		E-catcher
#6-4			38		Go1NET-3
#6-5			54		Go1NET-3
#7-1	1686	43.12	22	granite	E-catcher
#7-3			38		Go1NET-3
#7-5			86		Go1NET-3

Notes: Number denotes the number of monitoring stations. Elev. denotes the elevation; Depth denotes the depth perpendicular to the land surface; Lithology denotes the lithology of bed rock.

Table 2 The ground motion parameter characteristics in East-West (EW), North-South (SN) and Vertical Direction (VD). PGA = peak ground acceleration.

Number of monitoring station	PGA (cm·s ⁻²)			Topographic amplification factors		
	EW	SN	VD	EW	SN	VD
#1	82.29	85.86	74.67	6.69	8.02	8.68
#2	19.32	29.11	24.12	1.57	2.72	2.80
#6-5	10.25	10.09	20.78	0.83	0.94	2.42
#7-3	12.77	10.36	15.11	1.04	0.97	1.76

3 Discussion

3.1 PGA variation

Five monitoring instruments at different depths below the surface at the #6 adit were triggered during the Kangding Ms 5.8 earthquake and the recorded waveforms are shown in Figure 4. The characteristics of the seismic slope response are obtained from these monitoring data.

The values of the PGAs in all three directions are plotted against their depths below the surface in Figure 5, and these are plotted as ratios of the values at the tunnel entrance in Figure 6.

The trends of the peak acceleration ratio curves mirror the trends in the peak acceleration curves (Figure 5). The change law of the peak acceleration ratio curve is taken into account. Because the epicenter distance was approximately

43 km and PGA_V is usually bigger than PGA_H , the change law of the PGA_H is mainly discussed in the next part of this paper and is another reason that the horizontal amplification is most concerning for engineering. From Figure 5 and 6, it could be concluded that the ratio of the PGA_H acceleration decreases from the outside to the inside, and the value at the surface decreases more rapidly than those at depth, revealing a strong nonlinear attenuation law. The PGA_H at the innermost monitoring site (at 54 m perpendicular to the surface) was approximately half that of the outermost site, based on the monitoring data. What is more, the attenuation trend at the innermost station looks like it disappeared, meaning that the curve of the slope approaches zero. The results also confirm the analyses of the 192 reports of underground construction destructions during earthquakes (Sharma and Judd 1991), as well as the failure types and characteristics of the mountain tunnels during the Wenchuan earthquake (Li 2008). Shaking table tests show that acceleration amplification coefficients increase nonlinearly with increasing elevations, and generally reach a maximum at the slope surface and on its shoulders (Yang et al. 2012). Our research results are also in agreement with Yang's results, and all reveal the dynamic response of the slope from the outside to the inside in their measured monitoring data and shaking table tests. Although some qualitative conclusions can be agreed on, many more studies should seek quantitative parameters for future engineering designs. It is also important for us to understand the seismic landslides occurring at the ridges of mountains or at the middle and upper parts of a slope.

3.2 The acceleration response spectrum

The concept of the acceleration response spectrum is based on elastic system dynamics (Biot 1941). A series of response spectra curves are derived from a number of typical strong earthquake accelerations (Housner 1959). The response spectrum is a plot of the peak or steady-state responses (displacement, velocity or acceleration) of a series of oscillators of varying natural frequencies that are forced into motion by the same base vibration or shock, which is the

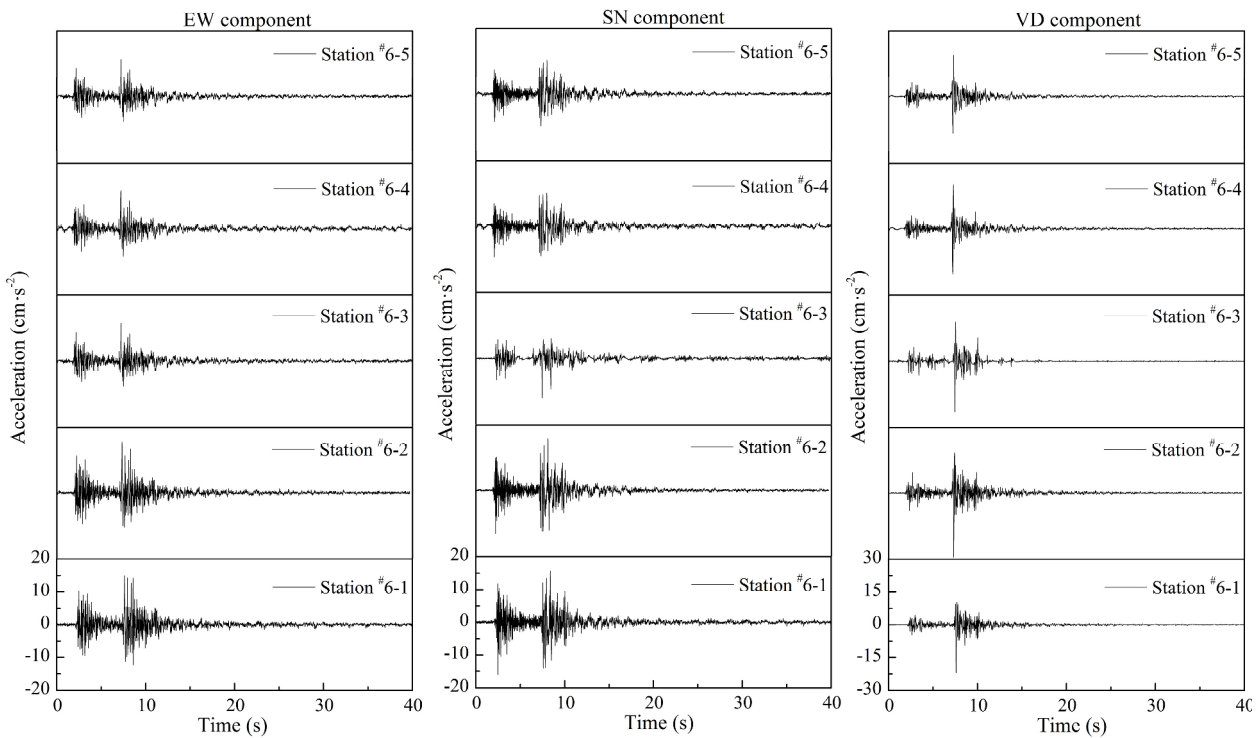


Figure 4 The waveform of each monitoring site in #6 adit.

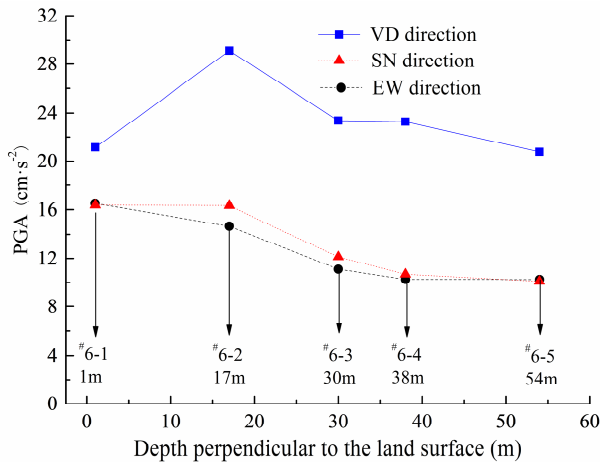


Figure 5 Peak acceleration of each monitoring site.

Abbreviations: PGA = peak ground acceleration; VD direction means Vertical direction; EW direction means East-West direction; SN means North-South direction.

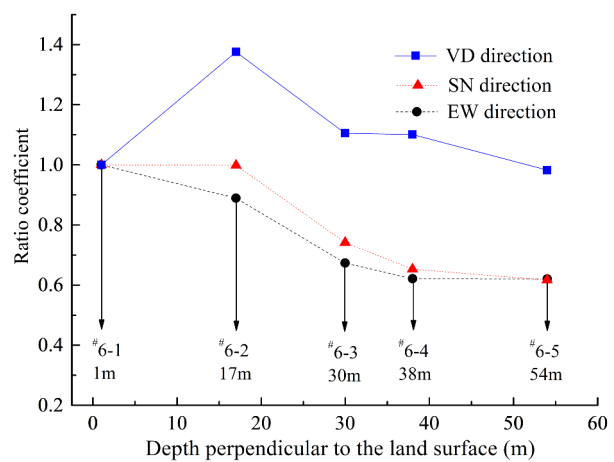


Figure 6 Peak acceleration ratio of each monitoring site.

essence of the reaction of the ground to seismic motions. According to the Chinese power industry standard called the specification of strong motion safety monitoring for hydraulic structures (DL/T 5416-2009), the horizontal acceleration response spectra with damping ratios of 5% are calculated, and the standard acceleration response spectrum is shown in Figure 7.

On the whole, the dynamic amplification factor of each monitoring point decays with an

increasing horizontal distance from the adit inwards. It decreases more rapidly near the surface and decreases only a little along the interior of the tunnel. Additionally, the response spectrum shape for the #6-1 monitoring point is significantly different to those of the other points, showing the effect of surface waves stimulated by body waves on the surface of the slope. The characteristic period of each monitoring point is concentrated from 0.1 to 0.4 seconds and shows that the energy

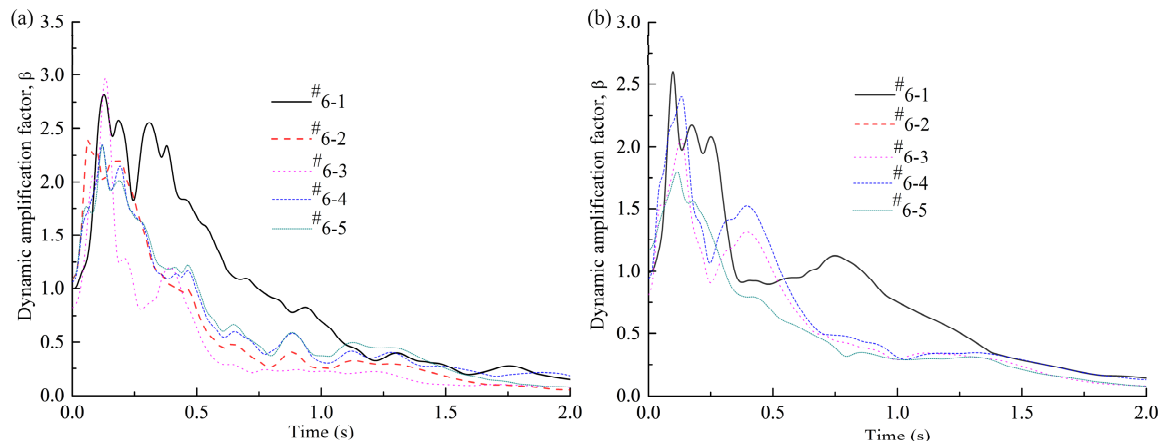


Figure 7 The horizontal acceleration standard response spectrum of each monitoring site: (a) EW direction; (b) SN direction.

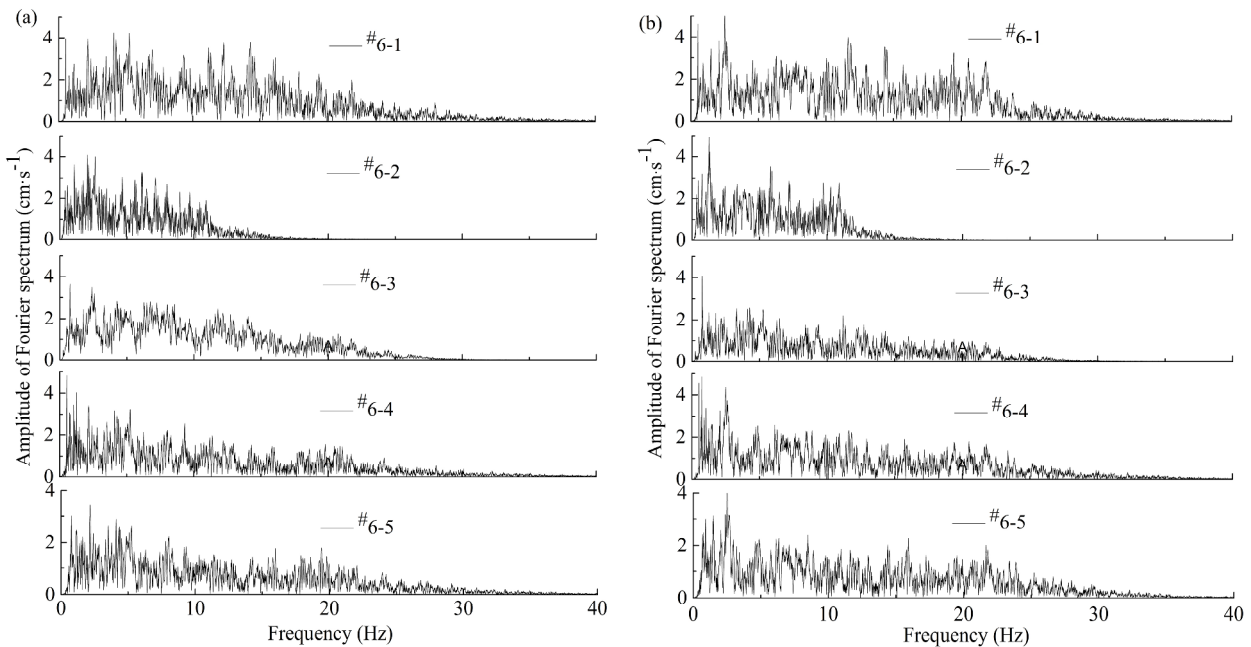


Figure 8 Fourier spectrum of each monitoring site: (a) East-West direction; (b) North-South direction.

is concentrated in the high frequencies. The response spectrum of each monitoring point substantially decreases with increased depth when the characteristic period is greater than 0.5 second. The spectra of the different monitoring points were generally similar to each other at periods greater than approximately 1.5 seconds.

3.3 Characteristics of the Fourier spectrum

The Fourier spectrum reveals seismic spectrum characteristics by transforming time to frequency. From the Fourier spectrum, the frequency components of ground motion and the

distribution of the energy of the ground motion at different frequencies can be inferred. The recorded monitoring data at the #6 station is transformed to the Fourier spectrum, and the Fourier amplitude spectrum at each monitoring point is calculated for different depths (see Figure 8); the maximum amplitude is shown in Table 3. The predominant frequency at each monitoring point is obtained, and the variation characteristics of the spectra at different depths from outside to the inside can also be studied.

The mean amplitude of the Fourier spectrum from the monitored points generally decreases from outside to inside, although the amplitude of

Table 3 Maximum Amplitude of Fourier spectrum

Number of monitoring station	Maximum Amplitude of Fourier spectrum(cm·s ⁻¹)		
	East-West	North-South	Mean
#6-1	4.24	4.92	4.58
#6-2	4.07	4.98	4.53
#6-3	3.59	4.08	3.84
#6-4	4.76	4.84	4.80
#6-5	3.46	4.41	3.94

the #6-4 monitoring point increases, and the numerical differences between each point are not obvious (see Figure 8 and Table 3). The Fourier spectra of the #6-1 point is complex and concentrated at higher frequencies; the amplitudes of almost all of the frequencies at this point are higher than those of the others and vary greatly due to the complex seismic waves at the surface. It also shows that the predominant frequency of each monitoring point is incomplete same and that some of these points even have several predominant frequencies, such as those concentrated at 5 to 15 Hz. It can be concluded that filtering is almost the same at the different parts of the slope with the same attitudes and that the range of amplification frequencies are similar.

However, above all, the seismic wave is magnified selectively in different parts of the slope at the same attitudes, and the amplification effect is weakened at greater depths. The elevation of the #6 monitoring station is approximately 110 meters above the bottom of the valley, and the peak reference acceleration is close to the #6-5 monitoring point; therefore, the amplification effect along the elevation is consistent with the amplification effect from the inside to the outside of the slope.

3.4 Directional variation of seismic shaking energy

The site response directivity can be effectively analyzed by examining the directional variations of the Arias intensity (Ia) (Arias 1970). A new method, called the polar diagram of the Arias intensity (Ia), is carried out to note the directional effect of the shaking energy (Del Gaudio and Wasowski 2007, 2011). Based on the former method, Luo et al. (2014) find that the amplification at Weigan hill is clearly oriented transverse to the relief elongation. The calculated results are shown in Figure 9, and

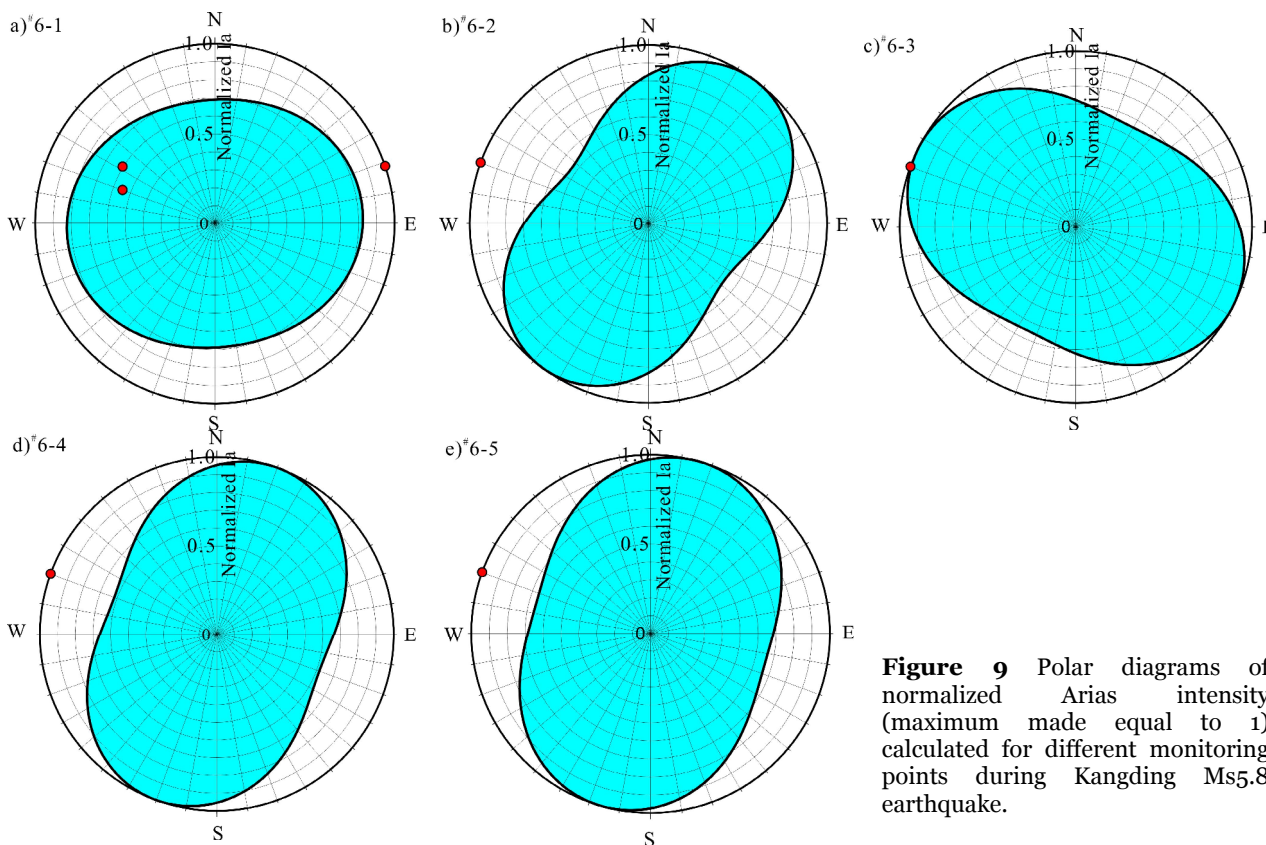


Figure 9 Polar diagrams of normalized Arias intensity (maximum made equal to 1) calculated for different monitoring points during Kangding Ms5.8 earthquake.

the event source back-azimuth (station-epicenter direction) is the same during the Kangding Ms 5.8 earthquake. The results clearly show that the Ia shape of the #6-1 point is an ellipse, while those of the others are close to the typical “peanut” shapes; thus, the site response directivity of #6-1 is weaker than those of the others. The differences revealed between the maximum and minimum Ia show that the maximum of point #6-2 is approximately 1 in the direction of N40°E and the minimum is 0.45 perpendicular to the maximum direction, while the maximum of point #6-4 is along N20°E, and that of point #6-5 is N15°E. However, the site response directivity of point #6-3 is not consistent with those of the other points, likely due to monitoring instrument layout error. As shown in Figure 9, the polar diagram of the normalized Arias intensity of point #6-1 is based on three different earthquake events that have different source properties, site-epicenter azimuths and propagation paths, which may lead to some ambiguous results compared with those of the other monitoring stations. However, it is found that the site response directivity is almost the same triggered when by one event. It may be concluded that the site response directivity was almost the same for different levels of depths at the same altitude.

3.5 Comparing data with simulation results

Various numerical simulation methods, including the finite difference method (Boore 1972), the Aki-Larner method (Bard 1982), and the indirect boundary elements method (Bouchon and Barker 1996), were used to better understand the seismic

responses of a slope. Recently, the FLAC3D software based on fast Lagrangian analysis of continua method was used to analyze the seismic responses of a slope and calculate the seismic stability of a slope, providing some practical and valuable results (Qi et al. 2003; Liu et al. 2004; Yan et al. 2013). In this section, FLAC3D is used to stimulate the seismic response of the geological prototype of the Lengzhuguan slope. The boundary setting, damping and input waves strictly obey the rules of the dynamic module of the FLAC3D software (Itasca Consulting Group 2005). The stimulation model is illustrated in Figure 10. Generally, the bottom width of the model is 1000 m, the left boundary height is 100 m, and the right boundary height is 650 m. In addition, many monitoring points are used to generate the acceleration time curve at a height of 230 m, which is same as the actual slope attitude difference, as well as finding this for other heights. In this paper, the studied slope is considered to be composed of a homogeneous, isotropic and elastic material with a density of 2.71 g·cm⁻³, a bulk modulus of 60.9 GPa and a shear modulus of 31.4 GPa (from laboratory test).

The peak ground accelerations of these monitoring points were obtained using the FLAC3D FISH programming language. Thus, the ratio curves at different height were calculated below the ground surface at different depths (see Figure 11). From the figure, it could be concluded that the PGA decreases with increasing depth. However, the trend of the change of the monitoring data was different from that at the same height difference ($H = 130$ meters) in the simulation results, and the monitoring results decreased

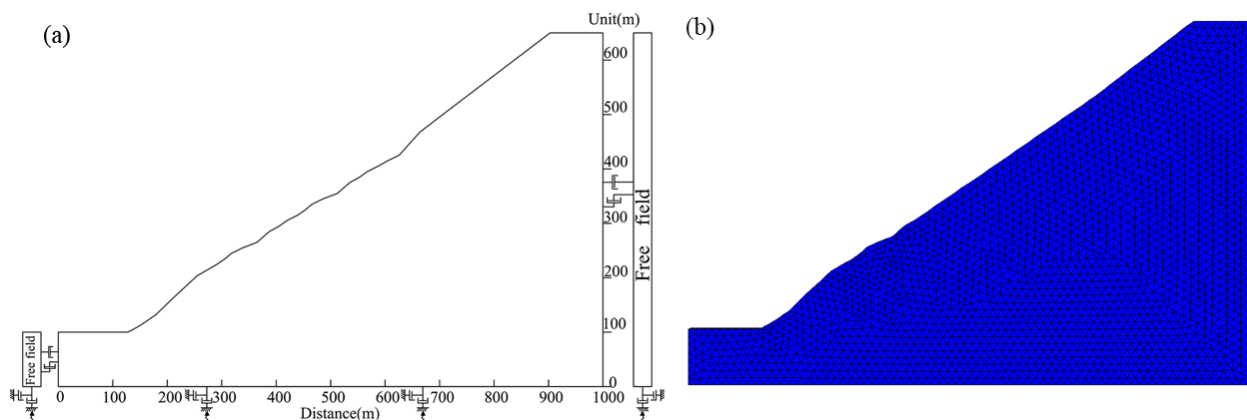


Figure 10 Schematic illustration of dynamic numerical simulation model of the slope: (a) simulation section and dynamic boundary setting; (b) FLAC3D meshing of the model.

sharply at the surface. It can be seen that the change law of the monitoring results was the same when the height difference was 300 meters. These differences might be due to the model used in the stimulation, differences in the physical and mechanical parameters or the rock structures. These factors will be considered in future numerical simulation studies.

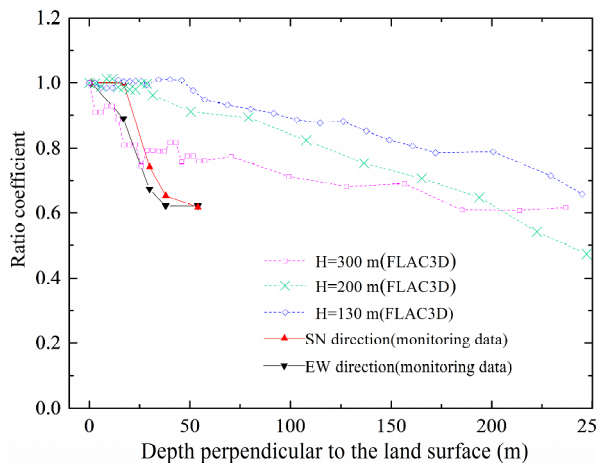


Figure 11 Stimulation results comparing with monitoring data (H , vertical height difference to slope toe).

3.6 Topographic amplification effects on slope stability

Many scholars have found that topographic amplification is a key factor in many coseismic landslides (Sepúlveda et al. 2005a; Sepúlveda et al. 2005b; Hough et al. 2010; Luo and Wang 2013). A simplified method was proposed to evaluate the seismic stability of steep slopes while considering the topographic effect (Ashford and Sitar 2002). Therefore, the topographic amplification effects should be considered when buildings or infrastructure, such as communication and power supply pylons, are built on various topographies or ridges. In this paper, some qualitative results are attained, but some quantitative design parameters are difficult to derive because of the lack of monitoring data. Some of the suggestions in this paper could be considered in engineering constructions in those mountainous areas in regions of high earthquake intensity, such as the Ya'an-Kangding highway in Sichuan province, southwestern China. Such constructions should not be built on steep cliffs and engineering measures such as shotcrete should be taken; moreover, different treatment measures can be taken in

different directions, according to the results of previous research.

4 Conclusions

Based on the seismic monitoring sections on the both sides of the Lengzhuguan gully, Sichuan Province, southwestern China, some data analysis results were presented in this paper. Data from 5 strong earthquake monitoring sites at the same elevations provided information on the change laws of the horizontal peak accelerations at depths below the surface. The data indicate that the peak horizontal ground acceleration decreases with increasing depth away from the adit portal, such that the horizontal ground acceleration innermost point is approximately 0.5 times that at the portal, and the variations with distance show a strongly nonlinear trend. Therefore, during the tunnel construction, the tunnel entrance is the main section in need of reinforcement.

The horizontal direction of the standardized acceleration response spectrum also indicates that the dynamic magnification coefficient of the acceleration response spectrum of each monitoring point is gradually reduced from the outside in, and the spectrum of the surface decreases much more than that at depth. The Fourier spectrum also shows the same change in trends as the PGAH and acceleration response spectra. The site response directivity was almost the same at different depths with the same altitudes.

Quantitative results are not available because of limited monitoring data, but some qualitative analyses can be used in evaluating the seismic stability of slopes and future engineering designs. In the future, many more seismic monitoring networks should be established for different geologies, geometries and lithologies to better understand the ground motion. Other research methods, such as shaking table test experiments and numerical simulations, should be combined to analyze this problem.

Acknowledgment

This study has been supported by the National Natural Science Foundation of China (51408086) and the Opening Fund of the State Key Laboratory of Geohazard Prevention and Geoenvironmental

Protection (Chengdu University of Technology) (SKLGP2015Z001). The authors express their

gratitude for the financial assistance.

References

- Arias A (1970) A Measure of Earthquake Intensity in Seismic Design for Nuclear Power Plants. MIT Press, Cambridge, Mass. pp 438-483.
- Ashford SA, Sitar N (2002) Simplified method for evaluating seismic stability of steep slopes. *Journal of Geotechnical and Geoenvironmental Engineering* 128: 119-128. [https://doi.org/10.1061/\(ASCE\)1090-0241\(2002\)128:2\(119\)](https://doi.org/10.1061/(ASCE)1090-0241(2002)128:2(119))
- Bard PY (1982) Diffracted waves and displacement field over two-dimensional elevated topographies. *Geophysical Journal International* 71(3): 731-760. <https://doi.org/10.1111/j.1365-246X.1982.tb02795.x>
- Biot MA (1941) A mechanical analyzer for prediction of earthquake stress. *Bulletin of the Seismological Society of America* 31(2): 151-171.
- Boore DM (1972) Note on effect of simple topography on seismic SH waves. *Bulletin of the Seismological Society of America* 62(1): 275-284.
- Bouchon M and Barker JS (1996) Seismic response of a hill: the example of Tarzana, California. *Bulletin of the Seismological Society of America* 86(1A): 66-72.
- Del Gaudio V, Wasowski J (2007) Directivity of slope dynamic response to seismic shaking. *Geophysical Research Letters* 34(12): L12301. <https://doi.org/10.1029/2007GL029842>
- Del Gaudio V, Wasowski J (2011) Advances and problems in understanding the seismic response of potentially unstable slopes. *Engineering Geology* 122(1): 73-83. <https://doi.org/10.1016/j.enggeo.2010.09.007>
- Geli L, Bard PY, Jullien B (1988) The effect of topography on earthquake ground motion: a review and new results. *Bulletin of the Seismological Society of America* 78(1): 42-63.
- He JX, Wang YS, Luo YH, et al. (2015) Monitoring result analysis of slope seismic response during the Kangding Ms6.3 earthquake. *Journal of Engineering Geology* 23(3): 383-393. (In Chinese) <https://doi.org/10.13544/j.cnki.jeg.2015.03.003>
- Hough SE, Altidor JR, Anglade D, et al. (2010) Localized damage caused by topographic amplification during the 2010 M7.0 Haiti earthquake. *Nature Geoscience* 3: 778-782. <https://doi.org/10.1038/ngeo988>
- Housner GW (1959) Behavior of structures during earthquakes. *Journal of Engineering Mechanics Division, ASCE* 85 (EM4): 109-129.
- Huang RQ, Wang YS, Pei XJ, et al. (2013) Characteristics of coseismic landslides triggered by the Lushan Ms7.0 Earthquake on the 20th of April, Sichuan Province, China. *Journal of Southwest Jiao Tong University* 48(4): 581-589. (In Chinese) <https://doi.org/10.3969/j.issn.0258-2724.2013.04.001>
- Itasca Consulting Group, Inc. (2005) *Fast Lagrangian Analysis of Continua in 3 Dimensions User's Guide, Version 3.0*.
- Jiang SP, Fang L, Lin Z (2014) Seismic response analysis of mountain tunnels in different depths. *Rock and Soil Mechanics* 35(1): 211-216, 225. (In Chinese) <https://doi.org/10.16285/j.rsm.2014.01.027>
- Li TB (2008) Failure characteristics and influence factor analysis of mountain tunnels at epicenter zones of great Wenchuan earthquake. *Journal of Engineering Geology* 16(6): 742-750. (In Chinese) <https://doi.org/10.3969/j.issn.1004-9665.2008.06.003>
- Liu CL, Qi SW, Tong LQ, et al. (2004) Stability analysis of slope under earthquake with FLAC3D. *Chinese Journal of Rock Mechanics and Engineering* 23:2730-2733. (In Chinese) <https://doi.org/10.3321/j.issn:1000-6915.2004.16.014>
- Luo DL, Gao B, Shen YS (2008) Research on simulating material of surrounding rock in tunnel seismic model experiment. *Journal of Shi Jiazhuang Railway Institute (Natural Science)* 21(3): 70-73. (In Chinese) <https://doi.org/10.13319/j.cnki.sjztdxzbzrb.2008.03.016>
- Luo XH (1988) *Research on earthquake engineering*. Seismological Press, Beijing, China. (In Chinese)
- Luo YH, Wang YS, He Yuan, et al. (2013) Monitoring result analysis of Lengzhuguan slope ground shock response of Lushan earthquake of Sichuan, China. *Journal of Chengdu University of Technology (Science & Technology Edition)* 40(3): 232-241. (In Chinese) <https://doi.org/10.3969/j.issn.1671-9727.2013.03.02>
- Luo YH, Del Gaudio V, Huang RQ, et al. (2014) Evidence of hillslope directional amplification from accelerometer recordings at Qiaozhuang (Sichuan—China). *Engineering Geology* 183: 193-207. <https://doi.org/10.1016/j.enggeo.2014.10.015>
- Luo YH, Wang YS (2013) A study on the mountain slope ground motion topography amplification effect induced by Wenchuan Earthquake. *Journal of Mountain Science* 31(2): 200-210. (In Chinese) <https://doi.org/10.16089/j.cnki.1008-2786.2013.02.012>
- Qi SW, Wu FQ, Sun JZ (2003) Dynamic response of slope. *Science China Technological Sciences* 33(B12): 28-40. (In Chinese) <https://doi.org/10.3321/j.issn:1006-9275.2003.z1.004>
- Qi SW, Wu FQ, Sun JZ (2003) General regularity of dynamic responses of slopes under dynamic input. *Science in China Series E Technological Sciences* 46: 120-132. <https://doi.org/10.1360/03ez0006>
- Qi SW, Wu FQ, Yan FZ, et al. (2003) *Rock Slope Dynamic Response Analysis*. Science Press, Beijing, China. pp 46-48. (In Chinese)
- Sepúlveda SA, Murphy W, Jibson RW, et al. (2005a) Seismically induced rock slope failures resulting from topographic amplification of strong ground motions: The case of Pacoima Canyon, California. *Engineering Geology* 80(3): 336-348. <https://doi.org/10.1016/j.enggeo.2005.07.004>
- Sepúlveda SA, Murphy W, Petley DN (2005b) Topographic controls on coseismic rock slides during the 1999 Chi-Chi earthquake, Taiwan. *Quarterly journal of engineering geology and hydrogeology* 38(2): 189-196. <https://doi.org/10.1144/1470-9236/04-062>
- Sharma S, Judd WR (1991) Underground opening damage from earthquakes. *Engineering Geology* 30: 263-276. [https://doi.org/10.1016/0013-7952\(91\)90063-Q](https://doi.org/10.1016/0013-7952(91)90063-Q)
- Shen YS, Gao B, Wang YX (2009) Structural dynamic properties analysis for portal part of mountain tunnel in strong earthquake area. *Chinese Journal of Rock Mechanics and Engineering* 28(Supp. 1): 3131-3136. (In Chinese) <https://doi.org/10.3321/j.issn:1000-6915.2009.z1.080>
- Wang CY (1987) Study on stability of the bank slope of Ertan Reservoir under seismic condition. In: *Problem of Rockmass Engineering Geomechanics, Vol.VIII*. Science Press, Beijing, China. (In Chinese)
- Wang CY, Wang SJ (1987) Research on seismic response of a slope on shaking table test. In: *Problem of Rockmass Engineering Geomechanics, Vol. VII*. Science Press, Beijing, China. (In Chinese)
- Wang YS, He JX, Luo YH, et al. (2015) Seismic monitoring of a slope to investigate topographic amplification. *International Journal of Geohazards and Environment* 1(3): 101-109. <https://doi.org/10.15273/ijge.2015.03.013>
- Yan Z, Gao L, Peng N, et al. (2013) Influence of ground parameters on the dynamic responses of anchored bedding rock slope. In: *AIP Conference Proceedings*. 1558(1): 2309-2312. <https://doi.org/10.1063/1.4826002>
- Yang GX, Wu FQ, Dong JY, et al. (2012) Study of dynamic response characters and failure mechanism of rock slope under earthquake. *Chinese Journal of Rock Mechanics and Engineering* 31(4): 696-702. (In Chinese) <https://doi.org/10.3969/j.issn.1000-6915.2012.04.007>
- Zheng YR, Ye HL, Xiao Q, et al. (2010) Seismic slope stability and tunnel analysis method based on full power analysis. *Journal of Disaster Prevention and Mitigation Engineering* 30 (Supp. 1): 279-285. (In Chinese) <https://doi.org/10.13409/j.cnki.jdpme.2010.s1.027>